NOTES AND CORRESPONDENCE

Design Considerations for a Network of Thermodynamic Profilers

J. A. SCHROEDER AND J. R. JORDAN

NOAA/ERL/WPL, Boulder, Colorado

M. T. DECKER

Cooperative Institute for Research in Environmental Sciences (CIRES), University of Colorado/NOAA, Boulder, Colorado

6 June 1988 and 22 March 1989

ABSTRACT

A modular design for a ground-based thermodynamic profiler is presented, based on experience with a six-channel microwave radiometer that has provided temperature, pressure, and moisture measurements continuously, unattended, since 1981. Each module consists of one pair of microwave channels, whose frequencies are chosen to facilitate the joint use of radio-frequency (RF) components, thus reducing hardware costs by nearly half. The number of modules included in a given system can be chosen to suit the altitude and accuracy requirements for that particular application. The accuracy of temperatures and pressure heights retrieved from simulated profilers with 4 to 18 channels is presented to illustrate the tradeoff between cost and accuracy.

1. Introduction

Ground-based microwave radiometric systems measure column-integrated water vapor and cloud liquid water content quite reliably. Heights of pressure levels and gross features of temperature and humidity profiles can also be retrieved from the ground-based measurements (Askne and Westwater 1986). Because of their automatic, continuous operation in nearly all weather conditions, these systems, known as thermodynamic profilers, may constitute one component of the next-generation weather observation network. The research profilers currently used, however, employ from 6 to 11 channels, resulting in costs that may render them impractical for an operational network.

Experience with the continuous, unattended operation of the Wave Propagation Laboratory (WPL) six-channel radiometric system at Stapleton Airport in Denver, Colorado led to design preferences for future systems required to operate in this mode, such as those in an operational network. We introduce here a modular radiometric system concept in which the number of channels and the channel frequencies can be chosen to minimize the cost of satisfying specific site requirements. We present hardware design considerations appropriate for a network of thermodynamic profilers and use the simulated performance of profilers with 4 to 18 channels to illustrate the tradeoff between accuracy and cost.

2. System components

The proposed profiler is composed of a combination of modules, chosen to satisfy specific site requirements.

Instruments that measure surface pressure (P), temperature (T), and relative humidity (RH) directly form the fundamental module, because they provide traditional information at low cost, and the measurements tie the inferred profiles to ground truth.

A two-channel moisture-sensing radiometer forms the second module. Instruments with one channel near the 22.235 GHz water line and a second channel in the absorption window near 30 GHz have proven capable of measuring precipitable water vapor, cloud liquid water content, and coarse humidity profiles (Hogg et al. 1983). In addition, information from this module can be used to correct other radiance measurements for moisture effects.

A third module, consisting of a channel pair in the 60 GHz oxygen absorption complex, provides temperature and pressure height information.

Additional modules might contain channel pairs chosen to enhance the accuracy of estimates obtained from any of the other modules. This investigation focuses on the potential of additional channel pairs in the 50 to 60 GHz region for reducing errors in temperature profile and pressure height estimation. Since channels between 50 and 53 GHz respond to water vapor as well as temperature, error reduction resulting

Corresponding author address: J. A. Schroeder, Thermodynamic Profiling Program, NOAA/WPL, 325 Broadway, Boulder, CO 80303.

from adding channels in this frequency range may be partially due to improved correction for water vapor.

3. Hardware considerations

Temperature control and packaging requirements make it more economical to house several radiometer channels together, rather than using separate housings for each channel. Because temperature control becomes difficult when more than two channels share the same housing, however, we present design considerations in terms of channel pairs.

In designing a network of profilers, an important concern is long-term calibration stability. The Dicke radiometers used by WPL since 1975 use an automatic gain control (AGC) circuit (Hogg et al. 1983). This design employs a separate mixer, intermediate frequency (IF) amplifier, and microwave switch for each frequency channel (Fig. 1a). This approach yields exceptional sensitivity and calibration stability over a three to six month period (Snider et al. 1988), but the cost of the millimeter-wave hardware necessary for this design is an obstacle to network implementation.

One approach to cost reduction is the shared microwave component design illustrated in Fig. 1b (Janssen 1987). This design also incorporates the AGC-corrected Dicke technique, but the components have wider bandwidths, and the mixer has multiple local oscillators that are switched sequentially among several different frequency channels.

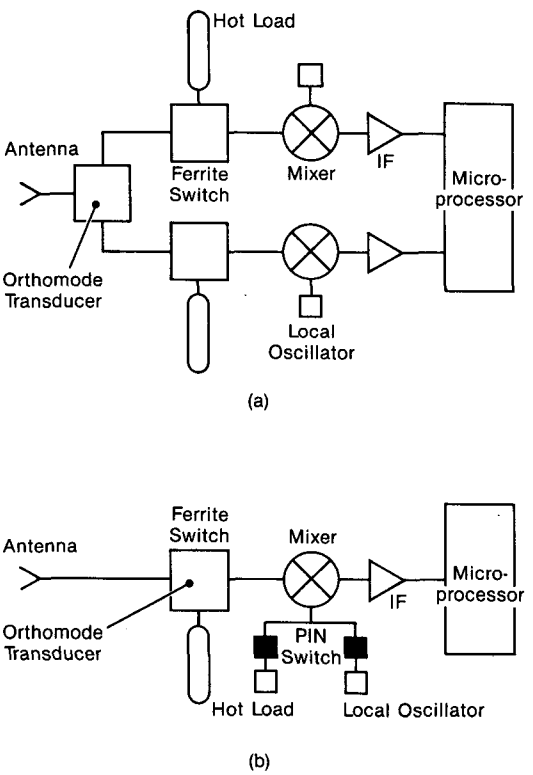

FIG. 1. Microwave components for a two-channel radiometer, using (a) traditional unshared design, (b) shared mixer design.

TABLE 1. Number of microwave components required for three radiometer designs, and relative cost for each design.

Component	Number required: Traditional four-channel	Shared four-channel	Shared two-channel
Antenna	2	2	1
Orthomode transducer	2	0	0
Hot load	4	2	1
Ferrite switch	4	2	1
Mixer/IF	4	2	1
Local oscillator	4	4	2
PIN switch	0	4	2
Microcomputer	2	2	1
Chassis	2	2	1
Relative cost	100%	50%	30%

Table 1 lists the hardware components necessary for three possible designs of a temperature/pressure profiling module. The relative costs shown for each design were obtained by multiplying the current purchase price of each component by the number required, adding the products, and dividing the sum by that of the traditional four-channel design. Labor costs were excluded. Hardware for a four-channel module constructed from two channel pairs that share components costs 50 percent less than hardware associated with the traditional four-channel design. Hardware for one pair of channels with shared components, which may suffice for lower tropospheric applications, costs 70 percent less than a traditional four-channel module. This dramatic cost reduction is due primarily to the reduced number of switches and mixers required by the shared-component design.

The reduction in cost, however, is accompanied by a reduction in sensitivity. In general, time-multiplexing multiple channels reduces the sensitivity by the square root of the fraction of time spent viewing the sky. For example, alternating between two channels will degrade the sensitivity by $\sqrt{2}$. Broadband mixers and switches have larger noise figures, which increase the receiver noise temperature, further decreasing sensitivity. However, ground-based profilers have the luxury of long integration times (30 s to 2 min), which compensate for sensitivity loss.

Switched ferrite circulators are currently the limiting factor in designing shared-component radiometers at these frequencies. Discussions with a switch manufacturer identified a 2 GHz bandwidth as the point at which a switch will start to degrade the data by 0.5 K, our assumed noise level. This constraint restricts the frequency locations of channels served by the same mixer to those separated by less than 2 GHz.

4. Simulation methodology

Computer simulations of radiometric and surface meteorology measurements were used to evaluate the performance of possible module combinations. All measurements were simulated from National Weather Service (NWS) radiosonde pressure, temperature, and moisture profiles above Denver, Colorado between 1970 and 1980. December, January, and February data were combined to represent winter conditions, and June, July, and August data together represented summer conditions. Surface P, T, and RH measurements were provided with the NWS soundings.

The theoretical relationship between the intensity of emitted radiation observed by the radiometers at the ground and the temperature, humidity, and pressure structure of the atmosphere is given by the radiative transfer equation

$$T_B = T_{bg} \exp\left[-\int_0^\infty a(h)dh\right] + \int_0^\infty T(h)a(h) \exp\left[-\int_0^h a(h')dh'\right]dh \quad (1)$$

where

T_B equivalent brightness temperature
T_{bg} cosmic background radiation
h height coordinate
$T(h)$ temperature at height h
$a(h)$ attenuation coefficient at height h

(Askne and Westwater 1986). At microwave frequencies, in the absence of heavy precipitation, scattering is small compared with absorption, so that $a(h)$ depends primarily on absorption by oxygen, water vapor, and clouds (suspended liquid water droplets).

Radiometer measurements (T_B) at frequencies of interest were simulated from each sounding by numerically integrating (1) with the NWS radiosonde measurements. We used Liebe's (1985) oxygen and water vapor absorption model to compute $a(h)$ as a function of pressure, temperature and moisture at level h. The resulting T_Bs represented radiometric measurements made during a wide variety of clear sky conditions.

Since radiosondes do not measure cloud liquid water content, we simulated liquid density distributions using the method of Decker et al. (1978). Within sounding layers where the RH exceeded 95 percent, they distributed three possible liquid densities, depending on layer thickness. The absorption by these liquid layers, calculated from the model given by Westwater (1972a), was added to the clear air $a(h)$. This cloud modeling scheme produced three additional T_Bs from each sounding in which the RH exceeded 95 percent. These T_Bs represented ground-based radiometer measurements made in the presence of many different cloud configurations.

Instrument noise was simulated by adding to each type of measurement Gaussian random errors with zero mean and standard deviations (σ) consistent with past observations made by WPL at Denver.

The continuous curve in Fig. 2 represents the root-mean-square (rms) difference between Denver radiosonde temperature measurements and those retrieved from the WPL six-channel thermodynamic profiler located at the radiosonde launch site (Askne and Westwater 1986). The rms differences were obtained from 460 profiles measured over a one-year period. The points marked × and ○ represent rms differences obtained for winter and summer, respectively, from simulated T_B measurements at the same six frequencies with σ = 0.5 K. The agreement demonstrated in the figure prompted us to use 0.5 K noise level for the simulated T_B measurements.

A statistical comparison between WPL and NWS surface P, T, and RH measurements revealed σ values of 0.3 mb, 0.5 K, and 4.4 percent. We chose these noise levels to represent realistic expectations of instrument performance in a network situation.

5. Channel selection

Assuming that surface P, T, RH measurements and a moisture-sensing module with channels at 23.87 and 31.65 GHz were part of the profiler system, we evaluated the impact of various combinations of oxygen channels between 50 and 60 GHz on the accuracy of retrieved temperature profiles and pressure heights. Channels between 60 and 70 GHz were avoided because of potential radio interference in all bands except the one between 64 and 65 GHz. In addition, the temperature weighting functions at these frequencies tend to replicate those between 50 and 60 GHz, due to oxygen absorption symmetry about 60 GHz.

Table 2 lists the secondary oxygen line frequencies between 50 and 60 GHz. We chose as radiometer channels the midpoint frequencies between lines, when the distance between lines could accommodate a double sideband receiver with a broad IF bandwidth for

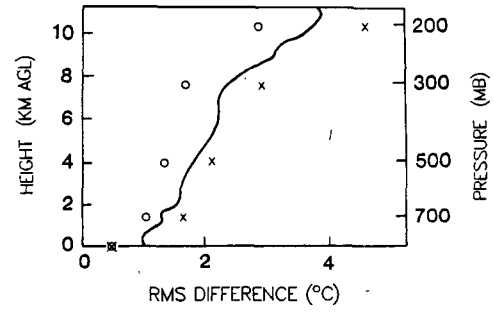

FIG. 2. Rms difference between radiosonde temperature measurements and those retrieved from WPL 6-channel Profiler measurements during 1982 (solid curve), simulated winter measurements (×), and simulated summer measurements (○).

TABLE 2. Secondary oxygen lines between 50 and 60 GHz (Liebe 1985), and midpoint frequencies used for simulations. Asterisks (*) mark midpoint frequencies omitted from the simulations.

Oxygen line (GHz)	Distance between lines (MHz)	Midpoint frequency (GHz)
49.96		
	510	50.30
50.47	520	50.73
50.99	510	51.25
51.50	520	51.76
52.02	520	52.28
52.54	530	52.85
53.07	530	53.33
53.60	530	53.85
54.13	540	54.40
54.67	550	54.94
55.22	560	55.45
55.78	480	56.02
56.26	100	56.31*
56.36	610	56.66
56.97	640	57.29
57.61	710	57.97
58.32	130	58.38*
58.45	710	58.80
59.16	430	59.38*
59.59	720	59.95*
60.31		

maximum sensitivity. The midpoint frequencies 56.31 and 58.38 GHz were eliminated because the distance between lines would require an undesirably narrow receiver bandwidth. Potential radio interference above 59 GHz eliminated the channels at 59.38 and 59.95 GHz. The 16 remaining oxygen channels were candidates for the temperature/pressure height module.

Temperature profiles and heights of the 700 and 500 mb pressure levels were obtained from the simulated measurements using the linear statistical retrieval technique of Westwater (1972b). The technique estimates the parameter of interest (e.g., temperature at height h) with a multiple linear regression equation in which the independent variables are the measurements. The coefficients obtained by regressing radiosonde measurements on simulated radiometer and surface measurements minimize the difference between the radiosonde measurements and the estimates. If the simulated measurements adequately represent actual measurements, the coefficients should produce equally accurate estimates when applied to actual measurements. We applied coefficients generated from 1970–75 radiosonde data to measurements simulated from 1976–80 radiosonde data, so that results would be analogous to those obtained by applying coefficients generated from a historical database to real-time measurements.

A useful technique for isolating the most effective independent variables in a multivariate regression equation is stepwise regression (Levenbach and Cleary 1984). In this study, we used stepwise regression to identify which oxygen channel combinations were the most effective estimators for each parameter, given the surface measurements and the 23.87/31.65 GHz radiometer measurements. The stepwise technique, however, could only identify the most effective channel combinations for a single parameter. For example, the best estimators for the 700-mb level temperature were not necessarily the best estimators for the 300-mb level temperature. Therefore, optimum frequency combinations for temperature profiling were not easily identified.

Figure 3 shows the temperature weighting functions for each of the 16 channels considered, in order of frequency. The rightmost curve corresponds to 58.80 GHz and the leftmost curve corresponds to 50.30 GHz. Each curve represents the change in T_B resulting from a 1-deg change in temperature over a 1-km layer at the altitude indicated. We avoided combining adjacent frequencies, because their weighting functions were so nearly duplicates. Correlations between simulated T_Bs at adjacent frequencies above 54.94 GHz and below 53.33 GHz exceeded 0.99 in both seasons.

Frequency allocation, stepwise regression, weighting functions, and hardware considerations together guided the order in which selected channels were added to the system to produce the best estimates with the fewest number of channels.

6. Simulation results

Because of the inversion technique employed, the results presented here depend on access to radiosonde soundings that adequately represent the thermodynamic profiler site climatology. We compare the temperature and pressure height estimates obtained from

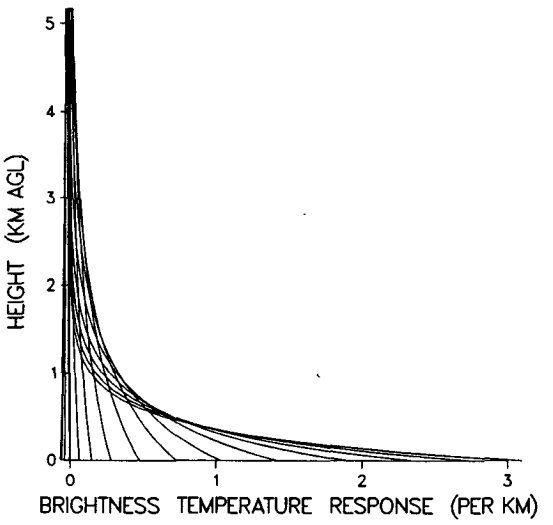

FIG. 3. Temperature weighting functions for the 16 channels given in Table 2. The leftmost curve represents 50.3 GHz and the rightmost curve represents 58.80 GHz. The x-intercept increases with increasing frequency, and the y-intercept decreases with increasing frequency.

the simulated measurements with corresponding radiosonde measurements.

The rms differences between radiosonde temperature measurements and the temperature estimated from one simulated hierarchy of successive channels appear in Fig. 4. The y-axis represents the first few kilometers above the ground, expressed as millibars of pressure above the surface. (The average surface pressure is 837 mb.) The x-axis shows the number of oxygen channels required to produce the rms temperature difference indicated on the vertical axis. The system corresponding to 0 channels consists of surface measurements and a radiometer with only the 23.87/31.65 GHz moisture channels. Each of the first two pairs of oxygen channels added, 57.29/55.45 and 54.40/52.85 GHz, could share radio frequency (RF) components. The order of the remaining 12 channels used to produce Fig. 4 is 50.3, 58.80, 56.66, 54.94, 53.85, 51.76, 57.97, 56.02, 53.33, 52.28, 51.25, 50.73 GHz. This figure is not intended to represent an optimum set of frequencies. Similar results were obtained with other combinations of channels. This is one example that satisfies the 2 GHz constraint on frequency separation for the first two pairs of oxygen channels added.

Figure 4 illustrates a rapidly diminishing return on investment. In the first 120 mb above the surface [about 1 km above ground level (AGL)], the first pair of channels removed more than 90 percent of the temperature difference that all 16 channels removed. Between 1 and 2 km AGL, the first pair alone removed more than 80 percent. The first two pairs together removed more than 90 percent below 2 km and more than 80 percent up to 4 km AGL. As a point of reference, the functional precision of radiosonde temperature measurements has been reported as 0.86 K (Hogg et al. 1983).

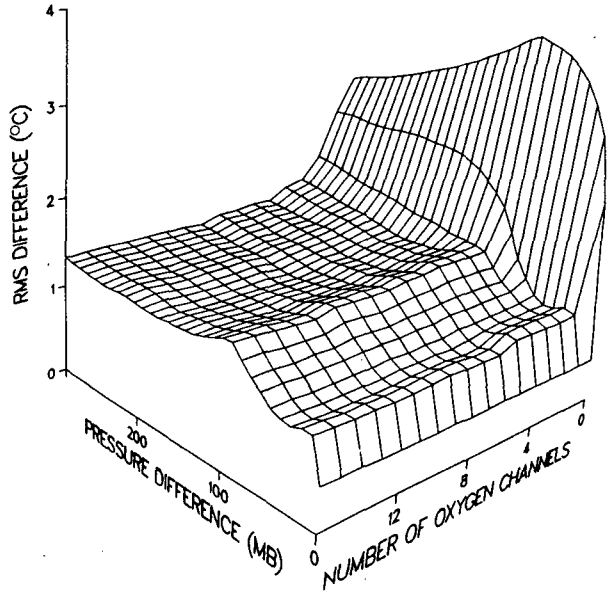

FIG. 4. Temperature differences between radiosonde and a thermodynamic profiler with the number of oxygen channels shown. The pressure difference axis represents mb above the surface at Denver, Colorado.

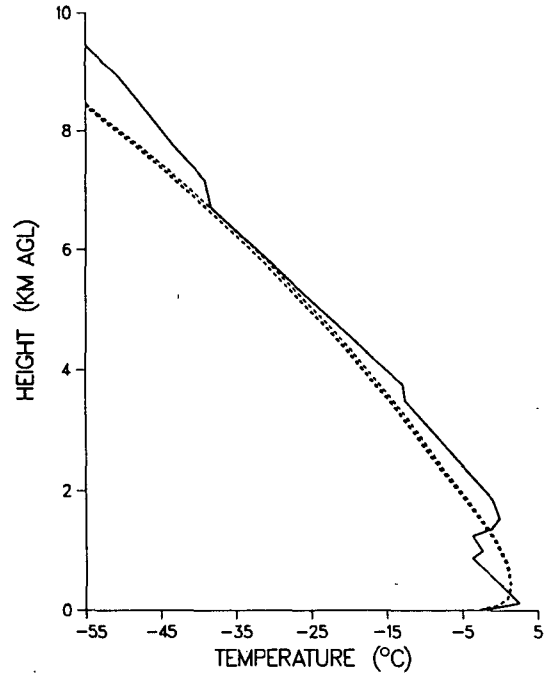

FIG. 5. Radiosonde temperature profile (solid curve) and temperature profiles retrieved from a simulated profiler with 2, 4, and 16 oxygen channels (dashed curves).

A major shortcoming of temperature profiles retrieved from radiometric measurements has been an inability to resolve elevated inversions. An example of a radiosonde temperature profile containing both ground-based and elevated inversions appears as the solid curve in Fig. 5. The three dashed curves, which are barely distinguishable, represent profiles retrieved from 2, 4, and 16 oxygen channels, respectively. Clearly, the additional channels do not provide the vertical resolution required in this case.

The rms differences for pressure heights (Fig. 6) exhibit a trend that is similar to the temperature results (Fig. 4). The functional precision of radiosonde 700 and 500 mb pressure height measurements, after correction to Denver surface pressures (Westwater et al. 1985), appear as a + on the respective curves in Fig. 6. The rms difference achieved with 2 and 3 oxygen channels matches the raob precision for 700 and 500 mb height measurements, respectively. Additional channels have little impact on accuracy.

7. Summary

The modular thermodynamic profiler described includes a surface meteorology module, a two-channel moisture-sensing module, and a pressure/temperature-

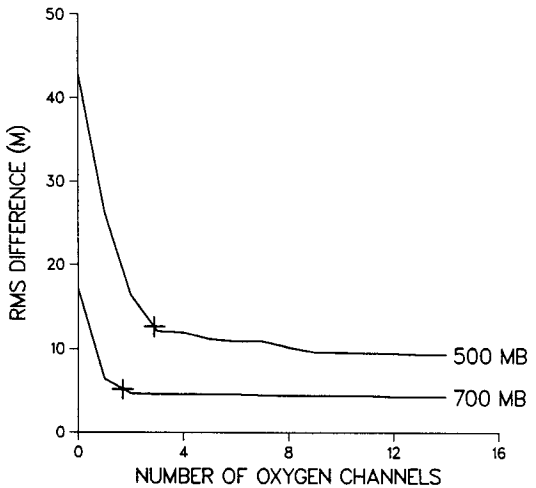

FIG. 6. Pressure height differences between radiosonde and a thermodynamic profiler with the number of oxygen channels indicated (solid curves); functional precision of radiosonde pressure height measurements (+).

profiling module with one or more channel pairs, depending on site requirements. The retrieval technique employed requires a priori knowledge of profiler site climatology.

Choosing channel pair frequencies to facilitate shared RF components reduces hardware costs by 40 to 50 percent, depending on the number of channels involved. Available switch technology limits the separation of channels that share components to 2 GHz, because a wider separation degrades measurement accuracy. If technological advancement removes the 2 GHz restriction, the frequencies of the first pair of channels in the temperature/pressure module could be located farther apart, resulting in better temperature accuracy over a wider altitude range.

Simulation results for Denver, Colorado indicate that, in the first few kilometers above ground, one pair of carefully chosen channels between 50 and 60 GHz, separated by less than 2 GHz, removes 77 to 97 percent of the temperature difference (error) removed by 16 channels in the same frequency range. The same single pair of channels provides heights of the 700 and 500 mb levels with accuracies comparable to radiosonde measurements. Temperatures retrieved from an 18-channel system exhibit the same coarse vertical resolution as those retrieved from a four-channel system. Therefore, the accuracy increment gained by adding successive pairs of channels between 50 and 60 GHz should be seriously weighed against cost, in the context of an operational network.

Acknowledgments. We thank E. R. Westwater of WPL for guidance and constructive criticism, M. J. Falls of WPL for radiosonde data, and both persons for software contributed for simulations. We also thank W. L. Eberhard of WPL for a thorough review of the manuscript.

REFERENCES

Askne, J. I. H., and E. R. Westwater, 1986: A review of ground-based remote sensing of temperature and moisture by passive microwave radiometers. *IEEE Trans. Geosci. Remote Sensing,* **GE-24**(3), 340–352.

Decker, M. T., E. R. Westwater and F. O. Guiraud, 1978: Experimental evaluation of ground-based microwave radiometric sensing of atmospheric temperature and water vapor profiles. *J. Appl. Meteor.,* **17,** 1788–1795.

Hogg, D. C., F. O. Guiraud, J. B. Snider, M. T. Decker and E. R. Westwater, 1983: A steerable dual-channel microwave radiometer for measurements of water vapor and liquid in the troposphere. *J. Appl. Meteor.,* **22,** 789–806.

Janssen, M. A., 1987: Data buoy microwave temperature sounder performance and evaluation, Final Report. JPL Rep. No. D-3865.

Levenbach, H., and J. P. Cleary, 1984: *The Modern Forecaster: The Forecasting Process Through Data Analysis.* Lifetime Learning Publications, 537 pp.

Liebe, H. J., 1985: An updated model for millimeter wave propagation in moist air. *Radio Sci.,* **20,** 1069–1089.

Snider, J. B., M. D. Jacobson, M. J. Falls and J. R. Jordan, 1988: Comparison of temperature profiles measured by three collocated microwave radiometers and radiosonde. NOAA Tech. Memo. ERL WPL-151, 39 pp.

Westwater, E. R., 1972a: Microwave emission from clouds. NOAA Tech. Rep. ERL 219-WPL 18, 43 pp.

——, 1972b: Ground-based determination of low altitude temperature profiles by microwaves. *Mon. Wea. Rev.,* **100,** 15–28.

——, W. Zhenhui, N. C. Grody and L. M. McMillin, 1985: Remote sensing of temperature profiles from a combination of observations from the satellite-based Microwave Sounding Unit and the ground-based Profiler. *J. Atmos. Oceanic Technol.,* **2,** 97–109.